Adsorption (2020) 26:973–987
https://doi.org/10.1007/s10450-020-00220-9

Modelling binary non-linear chromatography using discrete equilibrium data

Arvind Rajendran[1] · Rafael Teruo Maruyama[1] · Héctor Octavio Rubiera Landa[2,3] · Andreas Seidel-Morgenstern[2,4]

Received: 23 November 2019 / Revised: 9 February 2020 / Accepted: 13 March 2020 / Published online: 7 April 2020

Abstract

The determination and description of adsorption equilibria is critical for the design of several separation processes. In some instances, the dependence of the solid phase loading on the fluid phase concentration is complex and it is difficult to find a suitable functional form to represent the adsorption equilibria. This difficulty can be overcome by the use of discrete equilibrium data, i.e., using the experimental data of solid phase loadings and the corresponding fluid phase concentrations in its discrete form, without the use of a functional form to describe the adsorption isotherms. In this work we demonstrate how discrete equilibrium data can be used to predict binary competitive equilibria using the ideal adsorbed solution theory. Two approximations to generate data outside the range of measured values are proposed. The effectiveness of these methods in predicting competitive equilibria and elution profile of binary injections is demonstrated using numerical simulations. The application of this framework to estimate the regions of achievable separation for a multi-column simulated moving bed chromatographic separation is also discussed.

Keywords Adsorption column dynamics · Chromatography · Discrete equilibrium data · Ideal adsorbed solution theory

List of symbols

b	Equilibrium constant in Langmuir isotherm (L g^{-1})
c	Fluid phase concentration of solute (g L^{-1})
D_L	axial dispersion coefficient (cm^2 s^{-1})
H	Henry constant
L	Length of column (cm)
m	Dimensionless flow rate ratio
Pu	Target product purity (%)
Q	Volumetric flow rate (cm^3 s^{-1})
q	Solid phase concentration of solute (g L^{-1})
q^*	Solid phase equilibrium concentration of solute (g L^{-1})
t	Time (s)
t^*	Switch time (s)
v	Interstitial velocity (cm s^{-1})
x	Molar fraction on the solid phase
z	Axial coordinate (cm)

Subscripts and superscripts

D	Desorbent
E	Extract
F	Feed
i	Component
j	SMB section
R	Raffinate
sat	Saturation
tot	Total

Greek symbols

ε	Column void fraction

✉ Arvind Rajendran
arvind.rajendran@ualberta.ca

[1] Department of Chemical and Materials Engineering, Donadeo Innovation Centre for Engineering, University of Alberta, 9211-116 Street NW, Edmonton, AB T6G 1H9, Canada

[2] Max Planck Institute for Dynamics of Complex Technical Systems, Sandtorstr. 1, 39106 Magdeburg, Germany

[3] Georgia Institute of Technology, School of Chemical & Biomolecular Engineering, 311 Ferst Drive N. W., Atlanta 30332-0100, USA

[4] Otto-von-Guericke-Universität / Lehrstuhl für Chemische Verfahrenstechnik, Universitätsplatz 2, 39106 Magdeburg, Germany

1 Introduction

Adsorption and chromatographic separation processes exploit the ability of solids to selectively bind one or more components from a fluid mixture. The retention

characteristic of a particular species in a fixed-bed adsorber is described by its adsorption isotherm, that quantifies the partitioning of the adsorbate between fluid and adsorbent, i.e., solid phases, at a particular temperature. The estimation and mathematical description of adsorption isotherms is a critical step in designing adsorption-based separation and purification processes; these typically operate at relatively high concentrations, whereby each adsorbable component may potentially influence the adsorption behaviour of the other(s) (Ruthven 1984; Guiochon et al. 2006; Nicoud 2015).

Measurement of single component isotherms is rather straightforward; both static and dynamic methods are available (Seidel-Morgenstern 2004). In both liquid and gas phase measurements, when only a small sample of the adsorbent is available, e.g., at the adsorbent synthesis stage, static measurements are preferred. For single-component gas phase measurements static techniques such as gravimetry and volumetry are used, while in the liquid phase, the classical technique of batch adsorption is used (Ruthven 1984; Guiochon et al. 2006). Static measurements are highly automated and, in principle, a large-set of equilibrium measurements can be obtained in a straight forward manner. When a larger quantity of the adsorbent is available, and when processes are to be designed, dynamic measurements are performed (Seidel-Morgenstern 2004). In static methods, under controlled conditions the solid is exposed to a fluid mixture containing the solutes. Once equilibrium is attained, concentrations in the fluid phase, c_i, and corresponding equilibrium concentrations in the solid phase, $q_i^* = f(c_i)$, are either measured directly, or calculated indirectly using mass balances. Next, the fluid phase concentration is varied; a new equilibrium state is attained and measurements are repeated. This process is repeated until the desired concentration range is investigated. At the end of these investigations one ends up with a set of discrete points, relating q_i^* to c_i at a particular temperature, T, i.e., an adsorption isotherm. Among dynamic measurement methods, analysis of breakthrough curves, e.g., Frontal Analysis is widely applied (Lisec et al. 2001; Wilkins and Rajendran 2019). In this technique, a fixed-bed is initially equilibrated with a solvent or an inert carrier. Then, a step change in fluid phase concentration is introduced at the column inlet and the outlet concentration is recorded. An integration of the response curve, i.e., the recorded concentration profile of the outlet fluid stream, provides information about the single component loading. A single point on the isotherm can be calculated from this information. Other points of the isotherm can be obtained by repeating the experiment for different initial or feed concentrations. Before proceeding, it is worth highlighting that with advancements in molecular modelling techniques, it is also becoming increasingly common to obtain equilibrium points through in-silico simulations (Wilmer et al. 2012).

Once a set of equilibrium points is collected, a functional form, based either on a physical model of adsorption or an empirical formula is typically chosen and fitted to the experimental data (Guiochon et al. 2006). In practice, several models are tried and compared, before a suitable isotherm equation is finally selected. Models that can result in explicit competitive forms are naturally preferred as they simplify the computation of column dynamics. However, there remain situations where finding a suitable functional form to describe the equilibrium data is not straightforward. This is especially true for many novel materials such as metal-organic materials that exhibit properties that distinguish themselves from classical materials (Hefti et al. 2016). In order to describe the equilibrium data complex functional forms are chosen with multiple fitting parameters (Hefti et al. 2016; Pai et al. 2019). These functional forms are usually empirical and represent a "compromise" between accuracy of the fit and the complexity of the isotherm function. Further, owning to the many fitting parameters, the ability to extrapolate the isotherm beyond measured values remains uncertain.

Haghpanah et al. proposed a method to directly include discrete equilibrium data from static or dynamic measurements into computer simulations, circumventing the need to describe them using a smooth isotherm equation (Haghpanah et al. 2012). The key idea behind their approach is to describe any kind of complex single component adsorption equilibrium behavior without requiring a particular isotherm equation and use it to described fixed-bed column dynamics. They showed that single component breakthrough curves can be obtained with a high level of accuracy by using a sufficient number of discrete equilibrium data points and linear interpolation. It was also shown that discrete equilibrium points can be obtained by using the inverse method, where the equilibrium is determined based on elution profiles from pulse injections. The agreement with independently measured data and that obtained from the new approach was shown to be excellent. Other groups have also extended this idea (Forssén and Fornstedt 2015).

The main objective of the current work is to extend the approach developed by Haghpanah et al. to describe binary equilibrium and demonstrate its effectiveness for use in the simulation of binary non-linear chromatography. The approach of the discrete equilibrium data is briefly introduced and a proposal to use the ideal adsorbed solution theory (IAST) to describe competitive equilibrium data based on single-component discrete data is made. The effectiveness of this approach is evaluated using a case study and applied to the description of an experimental system. The potential of applying the approach to design multi-column simulated moving bed chromatographic processes is also considered.

2 Brief overview of discrete equilibrium data and IAST

2.1 Discrete equilibrium data

The concept of discrete equilibrium data relates to the representation of the thermodynamic phase equilibrium data in a discrete form, i.e., without the requirement of a functional form. This is illustrated in Fig. 1a where the equilibrium solid phase loading and the corresponding fluid phase concentration is represented by discrete markers that could be obtained through a suitable experimental technique. For concentrations, within the range where data is available, a simple linear interpolation between the bounding concentrations is used. In other words, the isotherm is represented by a piecewise linear function with knots at the positions where equilibrium data is available. This piecewise linear function can be easily incorporated into a numerical simulator in a straightforward fashion. To reiterate, the key advantage with this approach is that no functional form is required.

2.2 Ideal adsorbed solution theory

The IAST was introduced by Myers and Prausnitz (1965) to predict competitive adsorption equilibria from single component isotherms in the gas phase and extended to dilute liquid solutions by Radke and Prausnitz (1972). Let us consider the case of a binary adsorption of two solutes: the lighter component "1" and the heavier component "2". The phase equilibrium relationship is given by

$$c_1 = c_1^0 x_1 \tag{1a}$$

$$c_2 = c_2^0 (1 - x_1) \tag{1b}$$

where x_i is the solid phase mole fraction of component i, and c_i^0 is the fictitious concentration of component i at which the spreading pressures of the two solutes are identical. The equality of the spreading pressure in the case of a liquid phase can be represented, without loss of generality (Radke and Prausnitz 1972), by

$$\int_0^{c_1^0} \frac{q_1^*}{c_1} dc_1 = \int_0^{c_2^0} \frac{q_2^*}{c_2} dc_2 \tag{2}$$

For given values of c_1 and c_2, the above equations can be solved to obtain c_1^0, c_2^0 and x. Note that the integrals in Eq. 2 can be evaluated from single-component isotherms. These set of equations can be highly non-linear and the solution can be cumbersome in order to be incorporated into column dynamics simulations. Several approaches have been proposed in the literature to overcome the computational challenges (Landa et al. 2013; Mangano et al. 2015). Once the solution is obtained, the total loading of the two components q^*_{tot} can be obtained:

$$\frac{1}{q^*_{\text{tot}}} = \frac{x_1}{q_1^{*0}} + \frac{(1 - x_1)}{q_2^{*0}} \tag{3}$$

where q_i^{*0} is the pure component loading corresponding to c_i^0.

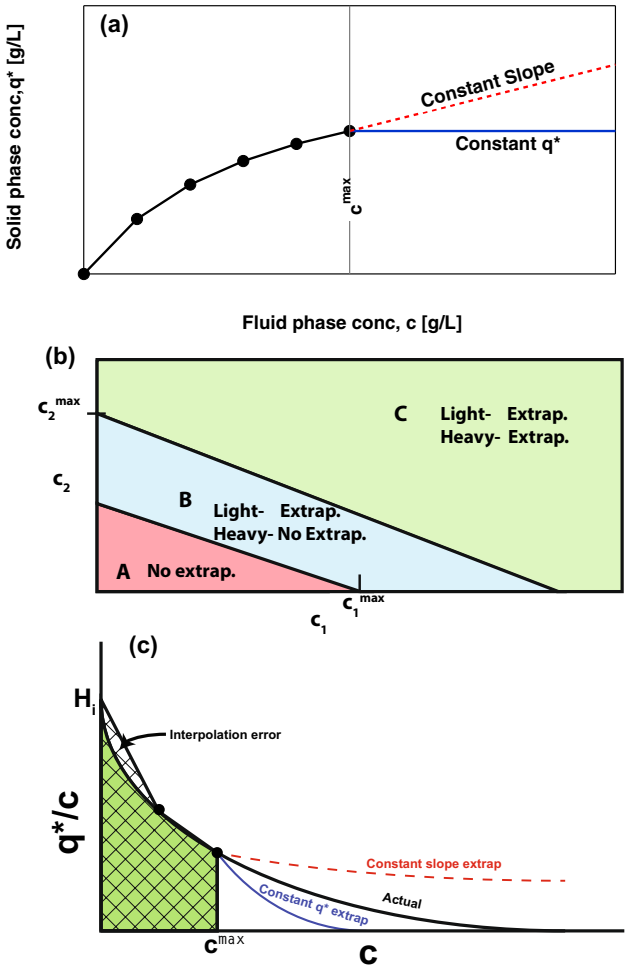

Fig. 1 Concept of discrete equilibrium data. **a** Illustration of discrete equilibrium data with five discrete points upto a maximum concentration, $c^{\max}$ and extrapolation techniques proposed. The black symbols represent discrete data, while the black lines show the piecewise-linear interpolation. The continuous blue line indicates the extrapolation based on constant q^* and the dotted lines represents that extrapolation based on constant slope. **b** The plot of the $c_1 - c_2$ plane showing the regions that require extrapolations during the calculation of competitive loading for the case of a Langmuir isotherm **c** Plot of the integral used to calculate the spreading pressure. The green region and the hatched regions show the contribution to the spreading pressure by the explicit function and the discrete equilibrium data, respectively (Color figure online)

Finally, the competitive equilibrium loadings, q_1^*, and q_2^* can be obtained from the following two equations:

$$q_1^* = q_{\text{tot}}^* x_1 \tag{4a}$$

$$q_2^* = q_{\text{tot}}^* \left(1 - x_1\right) \tag{4b}$$

Within the framework of the IAST where the isotherm is described using a functional form, Eq. 2, can result in a closed-form solution, making the solution rather straightforward (Tarafder and Mazzotti 2012). Where a closed form solution cannot be obtained, the integral is evaluated numerically. An essential requirement to apply IAST is the availability of single component adsorption equilibria in a sufficiently wide concentration range, since fictitious concentration values can become quite large for low values of x_i, i.e., $c_i^0 \gg c_i$. This is likely to occur for compounds that are either less adsorbed, or significantly diluted, e.g., traces, impurities (Mangano et al. 2015; Landa et al. 2013). Very often, especially in cases where the adsorption strengths of the two components are substantially different, the isotherm for the lighter component needs to be extrapolated significantly, possibly beyond values for which experimental measurements are available. The need for such an extrapolation can be illustrated by using the familiar Langmuir adsorption isotherm model which is given by:

$$q_i^* = q_i^{\text{sat}} \frac{b_i c_i}{1 + b_i c_i}, \quad i = 1, 2. \tag{5}$$

For the thermodynamically consistent situation with, $q^{\text{sat}} = q_1^{\text{sat}} = q_2^{\text{sat}}$, the solution of the IAST provides the closed form competitive form of the Langmuir isotherm:

$$q_i^* = q^{\text{sat}} \frac{b_i c_i}{1 + b_1 c_1 + b_2 c_2}, \quad i = 1, 2. \tag{6}$$

For a case where experimental data is available only upto maximum concentrations of $c_1^{\max}$ and $c_2^{\max}$, three regions can be identified on the $c_1 - c_2$ plane as shown in Fig. 1b. The two lines that separate the three regions are provided by the following two equations:

$$c_2 = -\frac{b_1}{b_2} c_1 + \frac{b_1}{b_2} c_1^{\max} \tag{7a}$$

$$c_2 = -\frac{b_1}{b_2} c_1 + c_2^{\max} \tag{7b}$$

In the figure, "A" refers to the region where no extrapolation of either isotherms are required; "B" to the one where only the light component isotherm needs to be extrapolated; and "C" to the one where both isotherms need to be extrapolated. It is worth noting that the IAST framework, requires extrapolation for both components, beyond the maxima of the measured concentrations, even if the concentrations encountered in the process might be less than the maximum values. Before proceeding to the implementation, it should be pointed out that not all systems can be adequately described by the IAST. Many aspects, including heterogeneity of the adsorbent, the nature of the adsorbate-adsorbent interactions, influence of the solvent, etc., can result in deviations from ideality. In such cases, the real adsorbed solution theory (RAST) could be invoked to alleviate some of the restrictions of the IAST (Myers 1983). In any case, the measurement of binary equilibria through appropriate experimental techniques is essential to validate the ability of these thermodynamic models to predict multi-component equilibria before proceeding to process design (Sircar 2006).

3 Incorporating IAST within the discrete equilibrium data framework

In the previous section, the IAST was introduced for situations where the isotherm is described by a functional form. Within the framework, the single component isotherms are used in evaluating the spreading pressure using Eqn. 2. In such a case, where the spreading pressure is evaluated numerically, only a smaller number of discrete values of q_i^*/c_i are required. Hence, discrete equilibrium data can be incorporated into the IAST in a rather straightforward manner. When doing so, two key challenges arise.

The first challenge relates to "interpolation". When a functional form is used, the summation form of Eq. 2, can be performed with practically infinite precision owing to the fact that the value of q_i^*/c_i can be calculated at any value of c_i. However, in the case of the discrete data loading information is available only at those values where experimental measurements are performed. Hence, the calculated spreading pressure is generally lower than the one with a functional form. The difference gets accentuated when only a few data points are available.

The second challenge is that of "extrapolation". When data is required only within region A (see Fig. 1), extrapolation is not required. However, when competitive loadings in regions B and C are required the extrapolation can be performed in a straightforward manner provided the functional form of the isotherm is available. In the case of the discrete equilibrium data, since there is no experimental information available beyond $c_i^{\max}$, there is no straightforward method for extrapolation. Suitable techniques have to be developed.

3.1 Effect of interpolation

Haghpanah et al, illustrated the impact of the number of experimental points on the ability of the discrete

equilibrium data to describe pulse elution profiles (Haghpanah et al. 2012). When a suitable number of points were available, excellent prediction of the profiles was possible. However, when fewer points were available, spurious oscillations occurred in the elution profiles and it was possible to link this to the "non-smooth" nature of the piecewise-linear form of the discrete equilibrium data. When considering IAST calculations, these errors also affect the estimation of the competitive loadings. This is illustrated in Fig. 1c, where the evaluation of the spreading pressure summation as seen in Eq. 2 is required. As seen in the same figure, the values of q_i^* are only available at discrete points. In the implementation of the summation, the trapezoidal rule could be used for calculating the areas. This approach will use a linear interpolation between adjacent values of q_i^*/c_i. For a Type 1 isotherm, this approximation will overestimate the area for c_i. Naturally, the error will reduce when additional discrete points are available. At this point, it is worth noting that for the purpose of integration, a linear interpolation of q_i^*/c_i will cause a lesser error in estimating the spreading pressure compared to using a linear interpolation of q_i^*.

In order to illustrate the error caused by interpolation, we consider a model system of two solutes that can be described by classical Langmuir isotherms:

$$q_i^* = \frac{q_i^{\text{sat}} b_i c_i}{1 + b_1 c_1 + b_2 c_2} \tag{8}$$

Specifically, we consider two systems, one which has a low non-linearity and the other that has a high non-linearity. For low non-linearity, we consider , $q_1^{\text{sat}} = q_2^{\text{sat}} = 10\,\text{gL}^{-1}$, $b_1 = 0.1\,\text{Lg}^{-1}$, $b_2 = 0.2\,\text{Lg}^{-1}$. For the high non-linearity system, we consider , $q_1^{\text{sat}} = q_1^{\text{sat}} = 10\,\text{gL}^{-1}$, $b_1 = 1\,\text{Lg}^{-1}$, $b_2 = 2\,\text{Lg}^{-1}$. Note that both systems have a selectivity of 2. The isotherm for both the systems are shown in Fig. 2 . In the case study,

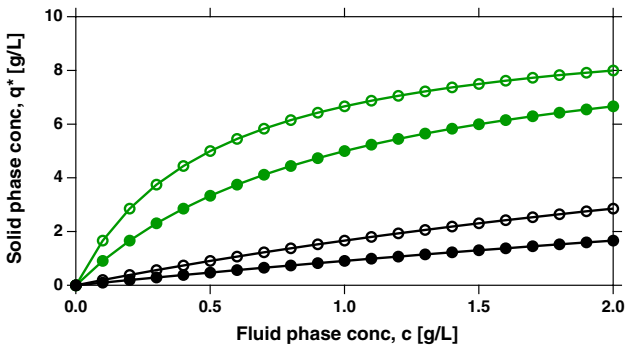

Fig. 2 Isotherms of the two discrete-equilibrium data systems used for the case studies. The green and the black symbols show the discrete data for the high non-linearity, and the low non-linearity systems, respectively. The open and closed symbols correspond to the heavy and light components, respectively (Color figure online)

we assume that five experimental discrete data points, i.e., $N = 5$, are available up to maximum concentrations of $2\,\text{gL}^{-1}$ and that the data points are spread evenly in this range. The goal is to evaluate the error that is caused in the calculation of the equilibrium loadings owing to the interpolation. The competitive loadings are calculated using the IAST approach described earlier. The error obtained for each solute is calculated as

$$E_i := \frac{q_i^* - \hat{q}_i^*}{\hat{q}_i^*} \times 100\% \tag{9}$$

where q_i^* and $\hat{q}_i^*$ are the competitive loadings calculated using the discrete equilibrium data and the explicit Langmuir isotherm provided in Eq. 8.

The contours of the error for the two systems is depicted in Fig. 3. The red triangle depicts the region A, i.e., where no extrapolation is required for either component. In both systems, the interpolation errors result in the prediction of lower q_i^* values as compared to the explicit competitive Langmuir isotherms. Generally, the errors in the case of the low non-linearity are smaller than those observed for the high non-linearity system. In fact, the errors are more pronounced at the low concentration regions. This is understandable as the $\hat{q}_i^*$ itself is quite small in this region and even a small error in the calculation of q_i^* will result in a higher fractional error. Note that the magnitude of errors will reduce if the number of available discrete equilibrium data increases.

3.2 Extrapolation strategies

As discussed above, in regions B and C, there is a need to extrapolate the isotherms to values beyond $c_i^{\max}$. In this work, we explore two simple extrapolation strategies, called **"Constant q*"** and **"Constant Slope"** that are defined as

$$\text{Constant q}^* : \quad q^*(c_i, c_i > c_i^{\max}) = q^*(c_i^{\max}) \tag{10a}$$

$$\text{Constant Slope} : \quad q^*(c_i, c_i > c_i^{\max}) = q^*(c_i^{\max}) + \frac{q_N^* - q_{N-1}^*}{c_N - c_{N-1}}(c_i - c_N) \tag{10b}$$

In the **"Constant q*"** strategy, the solid loading is assumed to be constant beyond $c_i^{\max}$ and is pegged to the value of q^* corresponding to $c_i^{\max}$. In the **"Constant Slope"** strategy the slope of the isotherm beyond $c_i^{\max}$ is set to be identical to that calculated from the last two points, $N-1$ and N, of the available data. The extrapolation strategies are shown in Fig. 1a.

At this point, it is worth discussing the impact of these assumptions. On the one hand, the **"Constant q*"** is

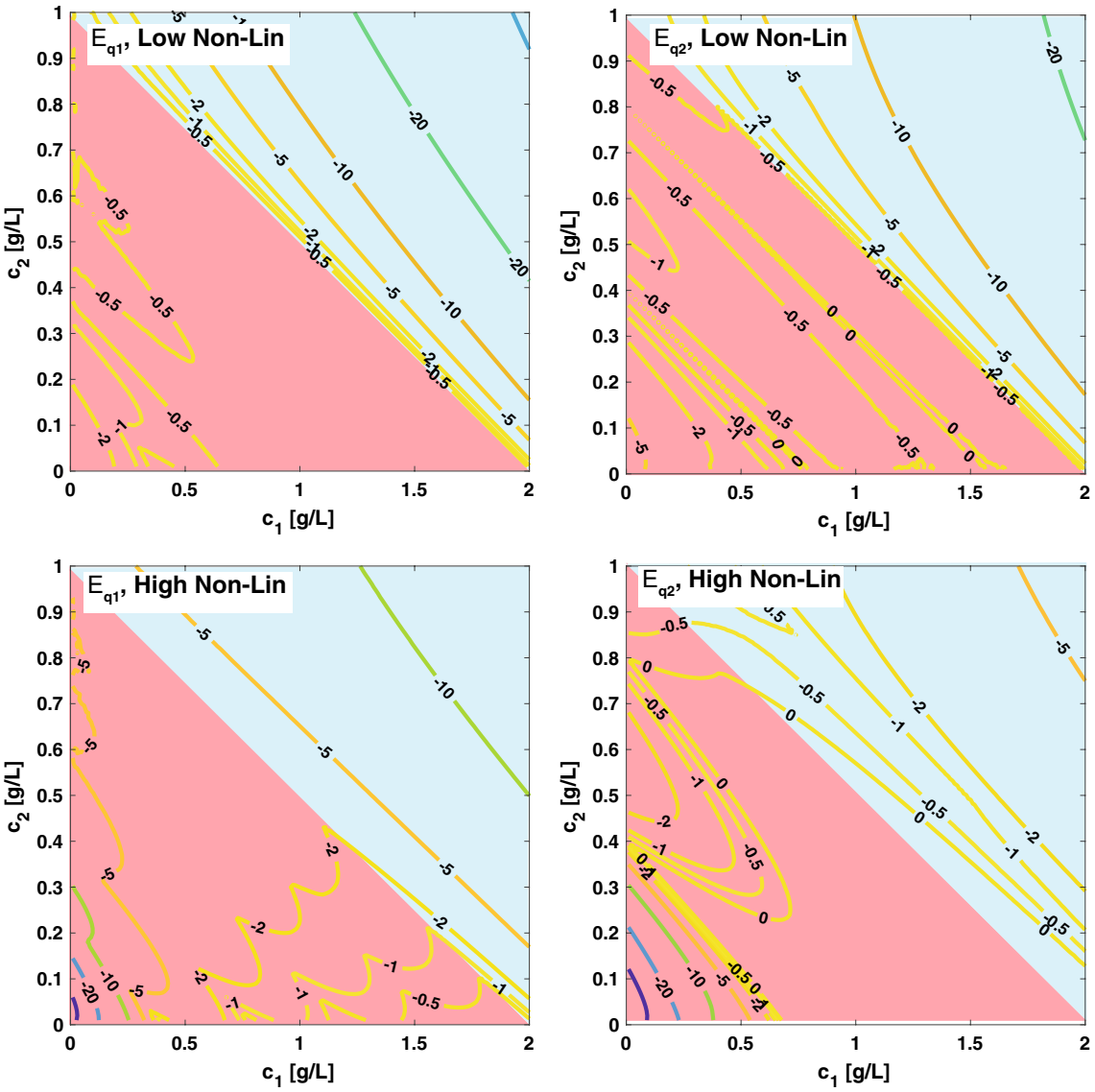

Fig. 3 Contour of the errors of equilibrium loading showing the impact of interpolation. In these cases 5 equally-spaced discrete equilibrium data was available between 0 and 2 g/L. The areas shaded with red and blue colours represent regions A and B as defined in Fig. 1b, respectively (Color figure online)

expected to be a good assumption if the available discrete equilibrium data is tending towards saturation. On the other hand, the **"Constant Slope"** is ideal for data that are closer to linear isotherms. Note that a preliminary estimate of this can be obtained by considering the magnitude of the local slope of the data. It is worth noting that other suitable extrapolations can be performed, for instance by fitting the existing data to any functional form. However, in the spirit of avoiding any functional description, we chose these two simple limiting approaches. As discussed in the earlier section, the use of IAST requires extrapolation of the isotherms. Figure 1c shows the effect of different extrapolation strategies. The fact that the capacity of an adsorbent is finite should require the value of q_i^*/c_i to approach zero as $c_i \to \infty$. While the Constant q^* extrapolation technique will comply with this requirement, the Constant Slope technique would not. For a Type 1 isotherm, the plot of q_i^*/c_i vs c_i is shown in Fig. 1c. Beyond $c_i^{\max}$, the Constant q^* extrapolation will underestimate the spreading pressure, while the Constant slope approach will overestimate it. At this juncture, it is worth pointing out that from a practical perspective, when an accurate picture of the adsorption phenomena is not known, any type of extrapolation beyond the vicinity of $c_i^{\max}$ is merely an approximate estimation. In liquid systems particularly, if $c_i^{\max}$ is near the solubility limit of the solute, any extrapolation is only hypothetical.

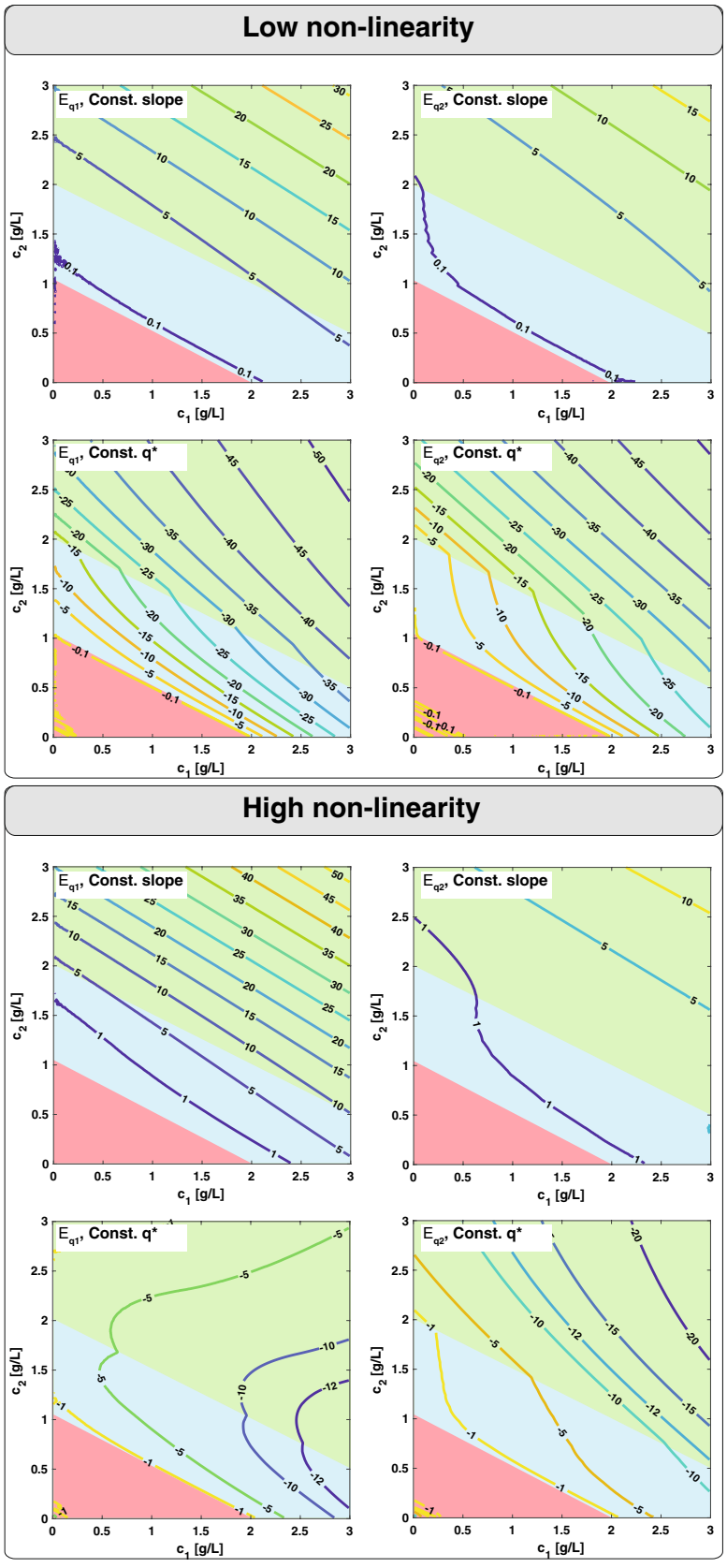

Fig. 4 Contour of the errors showing the impact of extrapolation using the two schemes, viz., Constant q^* and Constant Slope. In these cases 20 equally-spaced discrete equilibrium data was available between 0 and 2 g/L. The areas shaded with red, blue and green colours represent regions A, B and C as defined in Fig. 1b, respectively (Color figure online)

The errors caused by the two extrapolation strategies are illustrated in Fig. 4. For these calculations, since the goal was to study the effect of extrapolation techniques, we considered that there are 20 equally spaced points between 0 and 2 g/L for both components. Beyond 2 g/L, either of the two extrapolation strategies were employed. The low and high non-linearity systems show very different results. In the case of the low non-linearity case, the Constant slope extrapolation gives a better prediction, while the Constant q^* extrapolation works better for the high non-linearity system. The results are not surprising when considering that the high non-linearity system is indeed close to the saturation value at the conditions considered here. Summarizing, the choice of extrapolation technique should be based on the judgement of the available measured data.

Here, we have proposed two simple extrapolation techniques, that do not require any information about the competitive behaviour. In practice, it is quite possible that some form of information (either elution profiles or loadings) under competitive conditions is available. In such a situation, it is indeed possible to use other extrapolation strategies: for instance, the range beyond the last available experimental data point can again be discretized and these discrete points could be adjusted in order to describe the available experimental data, i.e., an approach similar to what was proposed for the single component (Haghpanah et al. 2012).

4 Simulation of chromatographic column dynamics

In the previous section, the errors associated with both interpolation and extrapolation were calculated. From a practical perspective it is important to understand how these errors translate into the prediction of chromatographic pulses. In order to do this the lumped kinetic model of chromatography is chosen. An axially-dispersed plug flow model is used and the column is considered to be isothermal. Under these assumptions the component mass balance can be written as

$$D_{L,i}\frac{\partial^2 c_i}{\partial z^2} - v\frac{\partial c_i}{\partial z} - \frac{\partial}{\partial t}\left[c_i + \frac{1-\varepsilon}{\varepsilon}q_i\right] = 0;\ i = 1,2 \qquad (11)$$

where $D_{L,i}$ is the axial dispersion coefficient, ε is the total column voidage, v is the interstitial velocity and q_i is the solid phase loading. The mass transfer between the fluid and solid phase is described by a linear driving force (LDF) model given by

$$\frac{dq_i}{dt} = k_i\left(q_i^* - q_i\right) \qquad (12)$$

where k_i is the LDF coefficient. In this work the chromatographic column is discretized along the axial direction into 100 cells using the Finite Volume Method. This transforms the PDEs into an ODE system to be integrated in time. The system of ODEs are then solved using the *ode45* solver in MATLAB, along with suitable initial and boundary conditions. In this work three chromatographic systems are considered. The specific dimensions and operating conditions are provided in Table 1.

The discrete equilibrium data is incorporated into the simulations in the following manner. The set of single-component equilibrium data, as available, is considered and for any value of the concentration less than the maximum available value, a piecewise linear interpolation is used. Beyond the maximum concentrations, based on the extrapolation method chosen, a sufficiently large number of equilibrium points are generated. Note that, once the single-component data is defined, the competitive loadings can be calculated at any arbitrary concentration pair, by solving the IAST as described above. Hence, the complete set of q_i^* is estimated and is fitted, a-priori, to a linear interpolant function available in Matlab called *griddedinterpolant*, that can be explicit for an arbitrary c_i. The interpolant function is then directly incorporated into the chromatographic simulations. This approach eliminates the solution of IAST at every node over the course of the temporal integration of the ODE system, thereby reducing the time required for solving the mass balance equations.

Table 1 Parameters used for the three systems in the simulation studies

Parameter	Langmuir system	TB system (Seidel-Morgenstern and Guiochon 1993)	SMB system
Length (cm)	25	25	10
Diameter (cm)	0.46	0.46	1
Voidage, ϵ (–)	0.59	0.66	0.59
Axial dispersion, D_L (cm^2/s)	3.0×10^{-3}	1.8×10^{-3}	3.0×10^{-2}
LDF coefficient, k, (1/s)	10	10	10
Volumetric flow rate (cm^3/min)	2	0.5	Various
SMB configuration	–	–	1/1/1/1

4.1 Simulation of a model system

At this point, we consider the effect of interpolation on chromatograms. In order to do this, a pulse injection of a 50:50 mixture of the two solutes is considered with the details provided in Table 1 and the caption of Fig. 5. Both low non-linearity and high non-linearity systems are considered.

For the purpose of studying the effect of interpolation, the injection concentrations were chosen in such way that all possible concentration states that will be formed within the column will stay within region A (red shade) in Fig. 3. Figure 5 shows comparisons of the chromatograms for both the low non-linearity and the high non-linearity cases. For the low non-linearity case, the match between the explicit form and the discrete data is excellent. Here, as seen from Fig. 3, errors arising from the discrete equilibrium data are rather modest. In the case of low concentration injections, the interaction between shock and wave transitions are weak and band broadening is controlled by dispersion. Hence, unless dispersion is strong, the feed concentration is not sufficiently degenerated. These phenomena contribute to a good representation of pulse dynamics, also using discrete equilibrium data. For the case of the high non-linearity system, while the position of shock fronts is predicted correctly, the overall prediction is less than desirable. Specifically, the mismatch is pronounced at low concentrations for the component 1. The match for the heavier component is rather good. This is in accordance with the errors observed in Fig. 3.

The effect of extrapolation on the ability to predict chromatographic pulses is shown in Fig. 5c, d. The difference between the discrete data points based calculation and that from the explicit form are quite pronounced in the case of the low non-linearity system. Specifically, the constant q^* extrapolation shows significant deviations from the actual profile as compared to constant slope extrapolation. As seen in Fig. 5, deviations for solute 1 are more pronounced than those for solute 2. The reason for this can be explained by considering the error that arises in the prediction of the loading. Note that the error in the estimation of the light component is always larger compared to the heavy component. This is indeed surprising, considering the errors seen in Fig. 4. However, this result can be rationalized by considering the dynamics of non-linear pulses in chromatographic columns. As it is well known, for the case of small volume injections under non-linear conditions, owing to wave interactions, the feed concentrations are eroded as the pulse propagates through the column. The higher the non-linearity, the more eroded is the feed concentration (Rajendran and Mazzotti 2011). This is

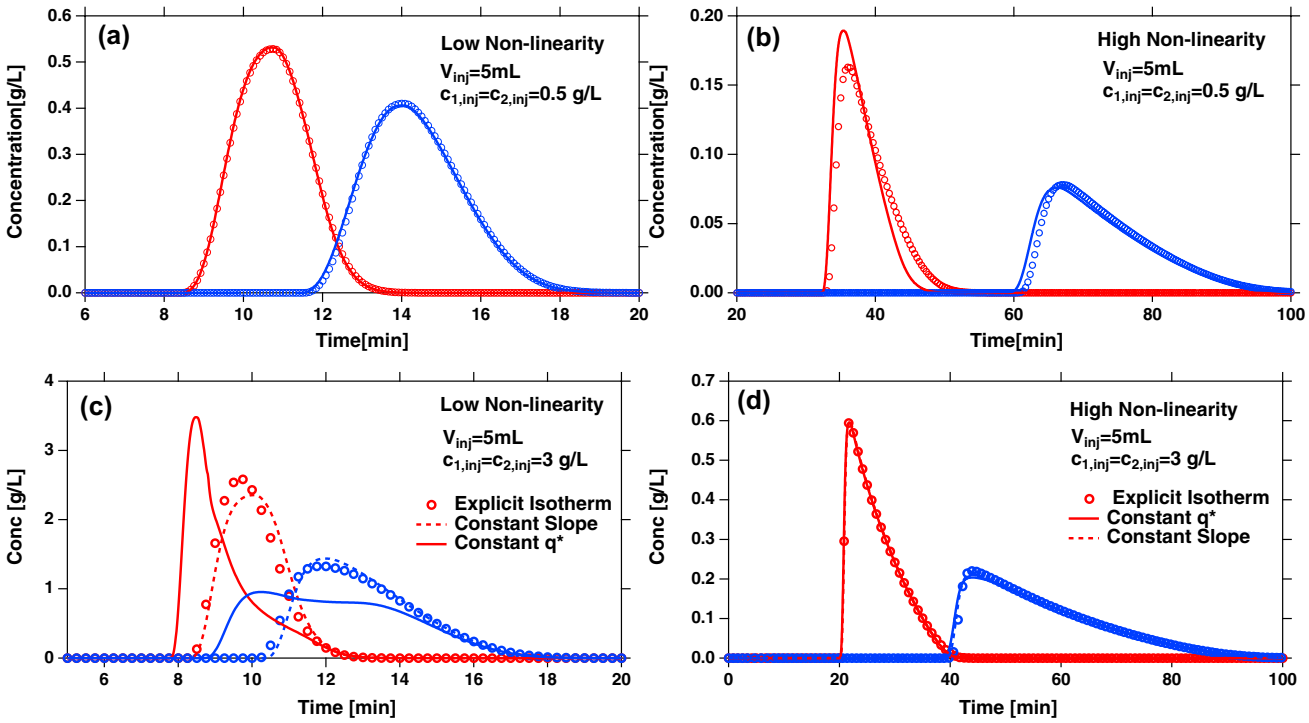

Fig. 5 Comparison of the chromatograms calculated using the explicit form and the discrete-equilibrium data. The top row shows the impact of interpolation and the bottom row shows the impact of extrapolation. **a**, **c** refer to the low non-linearity case, **b** and **d** refer to the high non-linearity case. In all figures, the symbols were from the explicit form. For the bottom row, the dashed and solid lines represent the Constant slope and Constant q^* extrapolation schemes

clearly seen in the chromatograms shown in Fig. 5 where the elution profiles for the two cases are very different.

4.2 Simulation of experimental pulse elutions

Seidel-Morgenstern and Guiochon reported the pulse elution of the enantiomers of Tröger's base (TB) on a microcrystalline cellulose triacetate with ethanol as the solvent (Seidel-Morgenstern and Guiochon 1993). The single-component and binary-injections were reported. Table 1 provides the details of the experimental conditions and additional model parameters. The isotherms of the two enantiomers were measured using single-component Frontal Analysis. A total of 23 points were collected for (+)-TB and 19 points for (−)-TB. This is a very interesting and challenging system in which (−)-TB exhibits a classical Langmuirian-type isotherm while (+)-TB exhibits an isotherm with an inflection point. Figure 6a shows the experimentally measured discrete equilibrium points and the plot of q^*/c for the two enantiomers. It is clear that (+)-TB exhibits an inflection point around 0.4 g/L. The authors used Langmuir and quadratic isotherms to model the single-component equilibrium behaviour of (−)-TB and (+)-TB respectively:

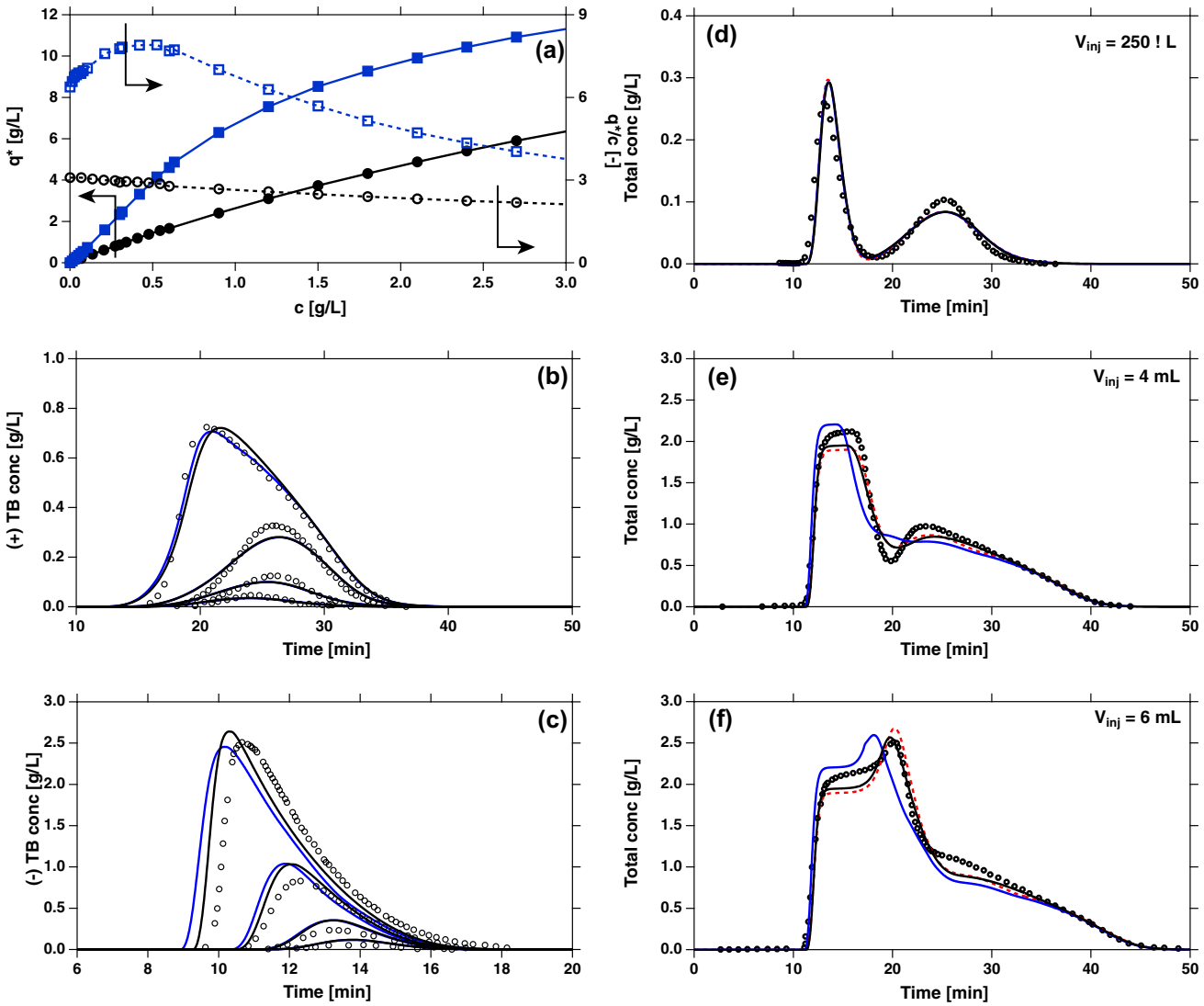

Fig. 6 Case study of the modeling of TB enantioners. **a** Experimentally measured discrete equilibrium data and the plot of q^*/c. **b** Experimental (symbols) and simulated elution profiles for (+)-TB enantiomer. Injection volumes were 10, 30, 90 and 250 µL. The injection concentration was 15 g/L. **c** Experimental (symbols) and simulated elution profiles for (−)-TB enantiomer. Injection volumes were 10, 30, 90 and 250 µL. The injection concentration was 15 g/L. **d–f** Binary injections of the two enantiomers with the injection concentration of each enantiomer being 1.5 g/L. The injection volumes are given in the inset. In all the elution profiles, the black, blue and the red curves represents the profile calculated using the explicit isotherm, the Constant q^* extrapolation strategy and the Constant slope extrapolation strategy, respectively (Color figure online)

$$\text{(-)-TB}: \quad q^* = \frac{3.09c_-}{1 + 0.157c_-} \tag{13a}$$

$$\text{(+)-TB}: \quad q^* = \frac{6.38c_+ + 14.43c_+^2}{1 + 0.948c_+ + 1.072c_+^2} \tag{13b}$$

Since at that time an explicit competitive form could not be found, they used the IAST to describe the multicomponent behaviour, numerically. Later, a closed-form binary equilibrium solution applying IAST was developed by Ilić et al. (2010).

The goal of this study was to use the data provided in the original paper and describe the pulse elution profiles using the discrete equilibrium data approach developed in this study. As an aside, it was important to point out that the original article used the equilibrium-dispersive model to describe the elution profiles and the current one uses a lumped kinetic model. Hence, a recalibration of the dispersion and mass transfer parameters was necessary and this was performed by fitting the elution profile using the detailed model to one of the published experimental profiles. The number of discrete equilibrium data points, measured experimentally, were retained.

Simulation results for the single-component elution are shown in Fig. 6 for both single component (sub-figures (b) and (c)) and the binary injections (sub-figures (d) to (f)) along with experimental profiles and calculations from the explicit isotherm. For the single component case, the match between the discrete equilibrium data and the explicit formulation is very good. In the case of the binary injections, for the lowest injection volume of 250 µL, the two extrapolation strategies are indistinguishable from the explicit form. For larger injection volumes, such as 4 and 6 mL injections, there is a clear difference between the two extrapolation strategies. Specifically, the Constant slope technique is much closer to the explicit form as compared to the Constant q^*. However, none of these formalisms, including the explicit form, are able to accurately describe the competitive behaviour. Note that the plateau formed in the 4 and 6 mL injections at around 2 g/L for the first component is a result of the roll-up (note that the injection concentration is only 1.5 g/L). None of the competitive forms predict this state accurately. While the explicit form and Constant slope underpredict this state, the Constant q^* overpredicts it. Nevertheless, this example showcases the potential of using discrete equilibrium data, in combination with the IAST, to also describe binary elution profiles for rather complex systems displaying inflection points.

5 Design of simulated moving bed chromatography

As a third and final case study, we explore the potential of the discrete-equilibrium data approach to predict the performance of a simulated moving bed chromatography (SMB) unit. The SMB is a well-known process that is used for the continuous chromatographic separation of a binary mixture (Rajendran et al. 2009; Nicoud 2015; Rodrigues 2015). The classical SMB consists of 4 sections (1 through 4). The solvent is introduced into Sect. 1; the extract (richer in heavy product) is removed between Sects. 1 and 2; feed is introduced in between Sects. 2 and 3; the raffinate (richer in light product) is removed between Sects. 3 and 4; and solvent is removed at the outlet of Sect. 4. Each section has a specific task: Sect. 1 to regenerate the solid phase; 2 and 3 to perform the separation; and 4 to regenerate the solvent. The main feature of SMB is the discrete periodic countercurrent movement of solid and fluid phases. The simulated movement is achieved by packing the stationary phase in fixed beds and sequentially switching the inlet and outlet ports in the direction of fluid flow. The SMB, and its variants, are commercially used, for example in enantiomer separations, sugar separations etc. (Nicoud 2015; Rodrigues 2015).

The performance of the SMB is governed by the dimensionless flowrate ratio m_j, which is defined as

$$m_j = \frac{Q_j t^* - V\epsilon}{V(1-\epsilon)} \tag{14}$$

where Q_j is the volumetric internal flow rate in section j, t^* is the switch time, V the column volume and ϵ the column void fraction (Mazzotti et al. 1997). The internal flow rates are related to the external flow rates through the following nodal balances:

$$Q_1 = Q_\mathrm{D} \tag{15}$$

$$Q_2 = Q_1 - Q_\mathrm{E} \tag{16}$$

$$Q_3 = Q_2 + Q_\mathrm{F} \tag{17}$$

$$Q_4 = Q_3 - Q_\mathrm{R} \tag{18}$$

Although the SMB is a fairly complex process, it is possible to understand (and design) the SMB using the separation regions plotted on the $m_2 - m_3$ plane. Provided the two conditions, $m_1 > H_2$ and $m_4 < H_1$ are met, the purity of the extract and raffinate can be identified on the $m_2 - m_3$ plane. It is worth noting that for the case of linear isotherms, these purity contours can be obtained analytically for the case of perfectly efficient columns (Rajendran 2008). For the case of low-efficiency columns and/or for the case of non-linear

isotherms these contours can be calculated using numerical simulations (Kaspereit et al. 2007; Maruyama et al. 2019). For SMB separations, the purity of extract and raffinate streams are calculated as:

$$Pu_{\mathrm{E}} = \frac{n_{2,\mathrm{E}}}{n_{1,\mathrm{E}} + n_{2,\mathrm{E}}} \tag{19}$$

and

$$Pu_{\mathrm{R}} = \frac{n_{1,\mathrm{R}}}{n_{1,\mathrm{R}} + n_{2,\mathrm{R}}} \tag{20}$$

where n denotes the number of moles of the product collected in a specific stream within one switch time.

The configuration of the SMB and the column dimensions used for this study are given in Table 1. The low nonlinearity system that was considered earlier in this work was considered for the SMB separation. It was assumed that 20 equally spaced equilibrium points were available upto $c_i^{\max} = 2$g/L. Beyond this point, the two extrapolation techniques discussed above were used. The values of the m_1 and m_4 were fixed at 10 and 0.1, respectively, and the $m_2 - m_3$ plane was discretized into a number of points. For each point on the $m_2 - m_3$ plane, the switch time was calculated using a minimum switch time method (Maruyama et al. 2019) and SMB simulations were carried out until cyclic steady state and the purities of the extract and raffinate streams were calculated. This was repeated for three different sets of feed concentrations, namely $c_1 = c_2 = 0.1$ g/L, $c_1 = c_2 = 1.0$g/L

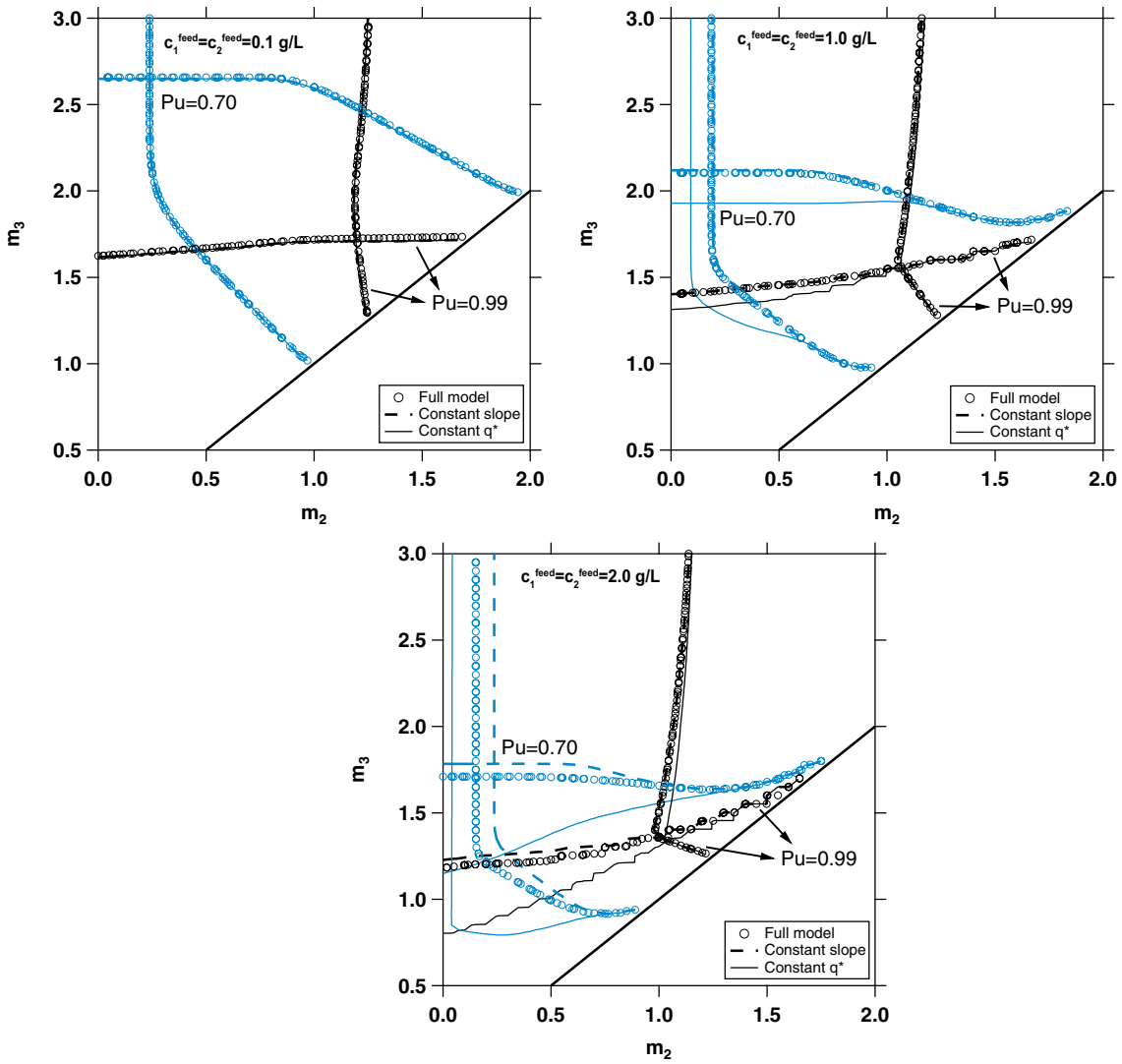

Fig. 7 Simulated moving bed chromatography (SMB) separation regions on the $m_2 - m_3$ plane for two different purities. The black symbols/lines refer to the case where an extract of raffinate purity of 99% is achieved, while the blue ones refer to the 77% case. The symbols indicate predictions from the explicit isotherm, the dashed and straight lines correspond to the ones from the Constant slope and Constant q^* extrapolation techniques, respectively (Color figure online)

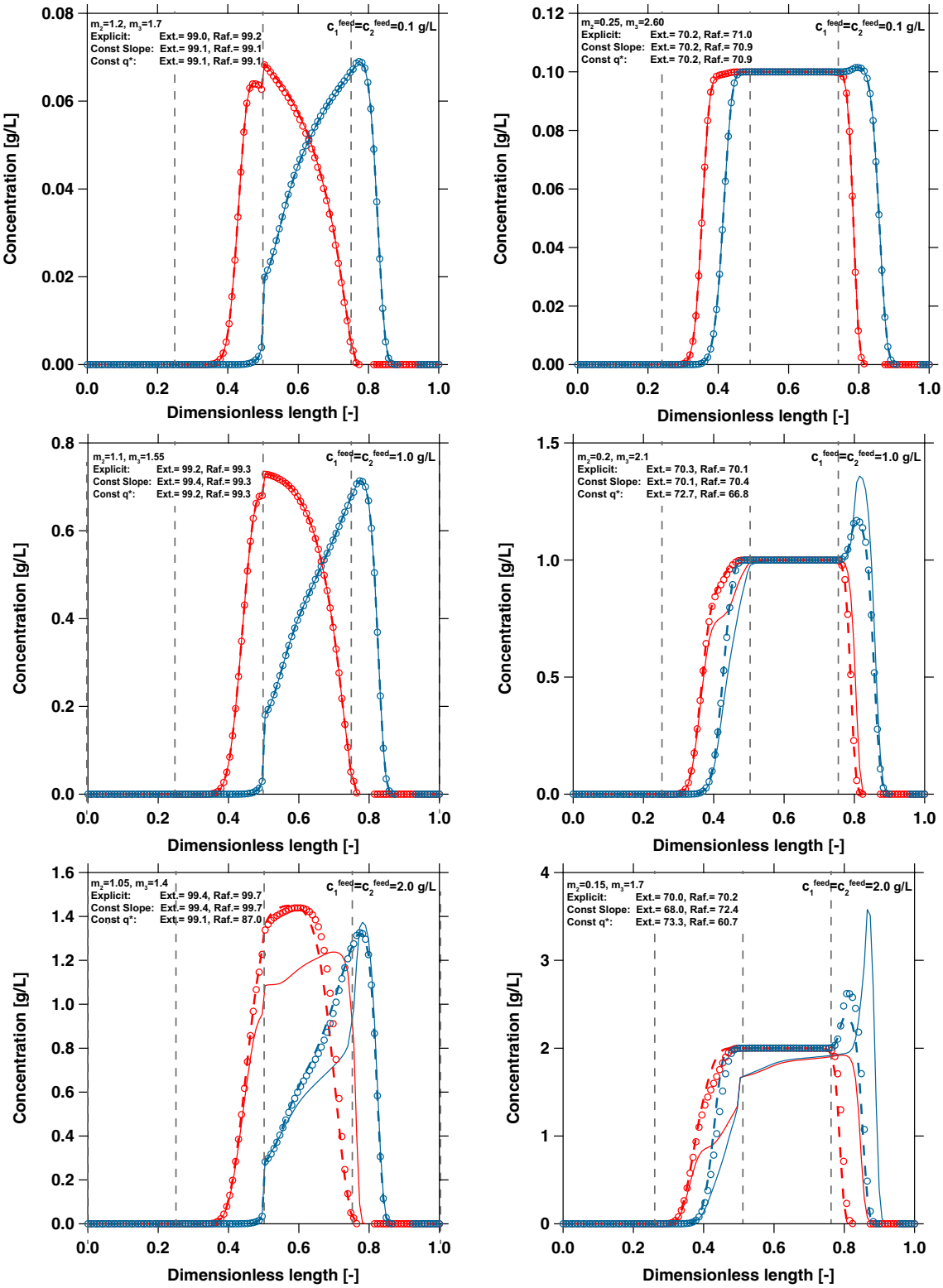

Fig. 8 Internal concentration profiles of the two components for cases where the raffinate and extract purities were ≈ 99% (left column) and 70% (right column). The red and the blue plots refer to the heavy and light component, respectively. The symbols indicate predictions from the explicit isotherm, the dashed and straight lines correspond to the ones from the Constant slope and Constant q^* extrapolation techniques, respectively. The specific values of m_2, m_3, feed concentrations and the purity/recovery values obtained from detailed simulations are provided in each sub-figure (Color figure online)

and $c_1 = c_2 = 2.0$ g/L. The purity contours are provided in Fig. 7. For the sake of clarity, only the contours of 99% and 70% purity are provided. At low concentrations, the contours predicted by the three approaches (explicit Langmuir, Constant slope and Constant q^*) virtually overlap with each other. At the intermediate concentration $c_1 = c_2 = 1.0$ g/L, the contours from Constant Slope extrapolation overlap with the explicit isotherm, while the Constant q^* shows deviation. It is worth noting that even under this situation, the region of complete separation, i.e., the space delimited by the 99% purity contour is well predicted by both extrapolation techniques. For the case of $c_1 = c_2 = 2.0$ g/L, while the 99% contour is predicted correctly by the Constant slope technique, there is a deviation for the 70% case. The Constant q^* extrapolation technique shows larger deviations.

The reasons for these deviations can be explained by considering the internal concentration profiles that are provided alongside each of the separation region plots for a specific operating condition shown in Fig. 8. At low concentrations, the prediction of the internal concentration profile is excellent. At higher concentrations, the deviation between the Constant q^* extrapolation (solid line) and the explicit form (symbols) start becoming obvious. The Constant slope extrapolation strategy works well in predicting the internal concentration profiles, while the Constant q^* extrapolation shows larger deviations, for the same reasons as discussed in the case of pulse elutions. It is worth noting that, unlike in the case of pulse injection, the feed state persists in the SMB case and the ability to predict the concentration profiles without applying an explicit isotherm is rather satisfactory.

6 Conclusions

This work provides a contribution to directly use discrete single component adsorption equilibrium points in order to generate a prediction regarding the equilibria in mixtures without applying an explicit single component isotherm model. For this the thermodynamically consistent ideal adsorbed solution theory (IAST) is applied. Effects and magnitudes of unavoidable interpolation and extrapolation errors are discussed and quantified. The method was demonstrated by describing adsorption dynamics in fixed-beds numerically, considering three different case studies of increasing complexity. In one of the case studies, a comparison with experimental data could be done. In the final case study, suitable operating conditions were predicted efficiently for the challenging multi-column simulated moving bed (SMB) chromatography process. As a key result of this work, we can recommend considering the direct processing of discrete single component equilibrium data as a suitable alternative for generating reasonable estimates of the courses of mixture separation processes. While we do not anticipate that this approach will provide any savings in computational time, it can be helpful for speeding-up process design and optimization, particularly to obtain preliminary results in order to decide upon the need for additional experimental efforts.

Before concluding, it is important to emphasize that the discrete equilibrium data that is proposed here should not be considered as a replacement to the time-tested methods of using thermodynamically consistent isotherm models that are based on the understanding of fluid-solid interactions. The ideal place to use such approaches are system that do not immediately lend themselves to an easy description by isotherm functions. Further, the discrete equilibrium data approach should be used with caution under the following situations:

1. Only a few discrete equilibrium points are available. Under these conditions, as shown here, significant errors can be expected.
2. The solutes show differences in their isotherm non-linearities. In this case, significant errors can be made in the estimation of competitive loadings.
3. When isotherms have been measured at concentrations much lower than where the process needs to be operated.
4. When significant errors are anticipated in the equilibrium measurements. In the case of using a functional form, some of these errors could be "smoothed-out", whereas in the current approach, they will show up as discontinuities. This can result in either numerical issues or produce spurious oscillations in elution profiles.

It is worth noting that many of the limitations remain as obstacles even when using explicit isotherms. This emphasizes the need for thorough experimental characterization of competitive adsorption prior to process development.

Acknowledgements Funding from Natural Science and Engineering Research Council, Canada through Discovery Grants program, Project Number RGPIN-2019-5018, is acknowledged.

References

Forssén, P., Fornstedt, T.: A model free method for estimation of complicated adsorption isotherms in liquid chromatography. J. Chromatogr. A **1409**, 108–115 (2015)

Guiochon, G., Felinger, A., Shirazi, S.G., Katti, A.M.: Fundamentals of Preparative and Nonlinear Chromatography. Academic Press, Boston (2006)

Haghpanah, R., Rajendran, A., Farooq, S., Karimi, I.A., Amanullah, M.: Discrete equilibrium data from dynamic column breakthrough experiments. Ind. Eng. Chem. Res. **51**(45), 14834–14844 (2012)

Hefti, M., Joss, L., Bjelobrk, Z., Mazzotti, M.: On the potential of phase-change adsorbents for CO_2 capture by temperature swing adsorption. Faraday Discuss. **192**, 153–179 (2016)

Ilić, M., Flockerzi, D., Seidel-Morgenstern, A.: A thermodynamically consistent explicit competitive adsorption isotherm model based on second-order single component behaviour. J. Chromatogr. A **1217**(14), 2132–2137 (2010)

Kaspereit, M., Seidel-Morgenstern, A., Kienle, A.: Design of simulated moving bed processes under reduced purity requirements. J. Chromatogr. A **1162**, 2–13 (2007)

Landa, H.O.R., Flockerzi, D., Seidel-Morgenstern, A.: A method for efficiently solving the IAST equations with an application to adsorber dynamics. AIChE J. **59**(4), 1263–1277 (2013)

Lisec, O., Hugo, P., Seidel-Morgenstern, A.: Frontal analysis method to determine competitive adsorption isotherms. J. Chromatogr. A **908**(1–2), 19–34 (2001)

Mangano, E., Friedrich, D., Brandani, S.: Robust algorithms for the solution of the ideal adsorbed solution theory equations. AIChE J. **61**(3), 981–991 (2015)

Maruyama, R.T., Karnal, P., Sainio, T., Rajendran, A.: Design of bypass-simulated moving bed chromatography for reduced purity requirements. Chem. Eng. Sci. **205**, 401–413 (2019)

Mazzotti, M., Storti, G., Morbidelli, M.: Optimal operation of simulated moving bed units for nonlinear chromatographic separations. J. Chromatogr. A **769**(1), 3–24 (1997)

Myers, A.L.: Activity coefficients of mixtures adsorbed on heterogeneous surfaces. AIChE J. **29**(4), 691–693 (1983)

Myers, A.L., Prausnitz, J.M.: Thermodynamics of mixed-gas adsorption. AIChE J. **11**(1), 121–127 (1965)

Nicoud, R.-M.: Chromatographic Processes. Cambridge University Press, Cambridge (2015)

Pai, K.N., Baboolal, J.D., Sharp, D.A., Rajendran, A.: Evaluation of diamine-appended metal-organic frameworks for post-combustion CO_2 capture by vacuum swing adsorption. Sep. Purif. Technol. **211**, 540–550 (2019)

Radke, C.J., Prausnitz, J.M.: Thermodynamics of multi-solute adsorption from dilute liquid solutions. AIChE J. **18**(4), 761–768 (1972)

Rajendran, A.: Equilibrium theory-based design of simulated moving bed processes under reduced purity requirements. linear isotherms. J. Chromatogr. A **1185**(2), 216–222 (2008)

Rajendran, A., Mazzotti, M.: Local equilibrium theory for the binary chromatography of species subject to a generalized langmuir isotherm. 2. Wave interactions and chromatographic cycle. Ind. Eng. Chem. Res. **50**(1), 352–377 (2011)

Rajendran, A., Paredes, G., Mazzotti, M.: Simulated moving bed chromatography for the separation of enantiomers. J. Chromatogr. A **1216**(4), 709–738 (2009)

Rodrigues, A.E.: Simulated moving bed technology: principles, design and process applications. Butterworth-Heinemann, Oxford (2015)

Ruthven, D.M.: Principles of Adsorption and Adsorption Processes. Wiley, New York (1984)

Seidel-Morgenstern, A.: Experimental determination of single solute and competitive adsorption isotherms. J. Chromatogr. A **1037**(1–2), 255–272 (2004)

Seidel-Morgenstern, A., Guiochon, G.: Modelling of the competitive isotherms and the chromatographic separation of two enantiomers. Chem. Eng. Sci. **48**(15), 2787–2797 (1993)

Sircar, S.: Basic research needs for design of adsorptive gas separation processes. Ind. Eng. Chem. Res. **45**(16), 5435–5448 (2006)

Tarafder, A., Mazzotti, M.: A method for deriving explicit binary isotherms obeying the ideal adsorbed solution theory. Chem. Eng. Technol. **35**(1), 102–108 (2012)

Wilkins, N.S., Rajendran, A.: Measurement of competitive CO_2 and N_2 adsorption on Zeolite 13X for post-combustion CO_2 capture. Adsorption **25**(2), 115–133 (2019)

Wilmer, C.E., Leaf, M., Lee, C.Y., Farha, O.K., Hauser, D.G., Hupp, J.T., Snurr, R.Q.: Large-scale screening of hypothetical metal-organic frameworks. Nat. Chem. **4**(2), 83 (2012)